NeuroImage 56 (2011) 1267–1275

Contents lists available at ScienceDirect

NeuroImage

journal homepage: www.elsevier.com/locate/ynimg

Focused ultrasound modulates region-specific brain activity

Seung-Schik Yoo [a,*], Alexander Bystritsky [b], Jong-Hwan Lee [a,c], Yongzhi Zhang [a], Krisztina Fischer [a], Byoung-Kyong Min [a], Nathan J. McDannold [a], Alvaro Pascual-Leone [d], Ferenc A. Jolesz [a]

[a] Department of Radiology, Brigham and Women's Hospital, Harvard Medical School, Boston, MA, USA
[b] Semel Institute for Neuroscience and Human Behavior, David Geffen School of Medicine, University of California, Los Angeles, CA, USA
[c] Department of Brain and Cognitive Engineering, Korea University, Seoul, Korea
[d] Berenson-Allen Center for Noninvasive Brain Stimulation, Department of Neurology, Beth Israel Deaconess Medical Center, Harvard Medical School, Boston, MA, USA

ARTICLE INFO

Article history:
Received 22 December 2010
Revised 1 February 2011
Accepted 17 February 2011
Available online 24 February 2011

ABSTRACT

We demonstrated the *in vivo* feasibility of using focused ultrasound (FUS) to transiently modulate (through either stimulation or suppression) the function of regional brain tissue in rabbits. FUS was delivered in a train of pulses at low acoustic energy, far below the cavitation threshold, to the animal's somatomotor and visual areas, as guided by anatomical and functional information from magnetic resonance imaging (MRI). The temporary alterations in the brain function affected by the sonication were characterized by both electrophysiological recordings and functional brain mapping achieved through the use of functional MRI (fMRI). The modulatory effects were bimodal, whereby the brain activity could either be stimulated or selectively suppressed. Histological analysis of the excised brain tissue after the sonication demonstrated that the FUS did not elicit any tissue damages. Unlike transcranial magnetic stimulation, FUS can be applied to deep structures in the brain with greater spatial precision. Transient modulation of brain function using image-guided and anatomically-targeted FUS would enable the investigation of functional connectivity between brain regions and will eventually lead to a better understanding of localized brain functions. It is anticipated that the use of this technology will have an impact on brain research and may offer novel therapeutic interventions in various neurological conditions and psychiatric disorders.

Introduction

The development of a non-invasive, anatomically-targeted method for the controlled modulation of regional brain activity would offer a new opportunity in creating a wide range of applications from functional brain mapping to the treatment of neurologic and neuropsychiatric disorders. Invasive techniques, such as deep brain stimulation (DBS), vagus nerve stimulation (VNS), and subdural and epidural cortical stimulation are finding increasing acceptance in neurotherapeutics (George and Aston-Jones, 2010; Hoy and Fitzgerald, 2010); however, these invasive methods accompany inevitable risks. As a non-invasive alternative to these invasive procedures, transcranial direct current stimulation (tDCS) and transcranial magnetic stimulation (TMS) have also been used to modulate cortical activity (Fregni and Pascual-Leone, 2007). Both modalities have shown the capability to either increase (via anodal tDCS or high frequency repetitive TMS) or decrease (via cathodal tDCS or repetitive TMS given in 1 Hz) the cortical excitability (Fregni and Pascual-Leone, 2007). These non-invasive methods, however, have limited spatial specificity and depth of penetration (Hoy and Fitzgerald, 2010; Wagner et al., 2007), impeding their broad application in brain research and in clinical neuroscience. Therefore, a new non-invasive modality that may overcome these limitations while providing sufficient control over the degree of regional neural excitability (i.e., *both* excitation and suppression) was sought after.

The use of ultrasound for functional neuromodulation has been demonstrated by several studies showing fully reversible inhibition of visual evoked potentials (Fry et al., 1958) and elicitation of auditory-nerve responses in cats (Foster and Wiederhold, 1978). A phenomenon, which resembled auditory stimulation, has been reported during the administration of transcranial Doppler ultrasound on the human brain (Magee and Davies, 1993). More recently, reversible excitation of the motor cortex has been demonstrated in the excised rodent brain tissue (Tyler et al., 2008) and live rodents (Tufail et al., 2010). These studies were based on the non-targeted deposition of unfocused acoustic beams to various neural structures; therefore, the induction of selective modulatory effects in a localized neural structure was not feasible. Focused ultrasound (FUS) techniques enable the delivery of spatially-confined acoustic energy to a small tissue region non-invasively, typically under the guidance of medical imaging techniques (Jolesz et al., 2005). By independently actuating multiple transducers arranged in a helmet-like fashion surrounding the skull, the location of the acoustic focus can be accurately controlled by a summation of

* Corresponding author at: Department of Radiology, Brigham and Women's Hospital, Harvard Medical School, 75 Francis Street, Boston, MA 02115.
E-mail address: yoo@bwh.harvard.edu (S.-S. Yoo).

1053-8119/$ – see front matter © 2011 Elsevier Inc. All rights reserved.
doi:10.1016/j.neuroimage.2011.02.058

ultrasound beams originating from the transducers (Clement et al., 2005).

Given the non-invasive ability to deposit steerable ultrasound energy to small areas located deep inside the brain, we were motivated to demonstrate that FUS can induce functional neuromodulation (i.e., both excitation and suppression) of regional cortical activity *in vivo* using an experimental animal (rabbit) model. We applied FUS, delivered as a train of pulses at low acoustic intensity (far below the level that will elicit tissue (Dalecki, 2004; Rinaldi et al., 1991)) to the animal's primary somatomotor and visual areas, as guided by anatomical and functional information from magnetic resonance imaging (MRI) and electrophysiological recordings.

Method and materials

Animal preparation

All animal procedures were conducted in compliance with the regulations and standards of the Institutional Animal Care and Use Committee. New Zealand white rabbits ($n=19$; all male, body weight 3.5–4.5 kg) underwent craniotomies prior to the sonication experiment. Although sonication can be delivered through the intact rabbit skull (~1.5–2 mm thick), the craniotomy was performed to allow for skull-free estimation of the ultrasound intensity at the sonication focus. Under the anesthesia of ketamine and xylazine (35 mg/kg and 10 mg/kg, respectively), a piece of skull (oval shaped, approximately 1.5×2 cm^2) was removed while leaving the dura intact, and the skin was sutured back over it. All of the animals, except for one, recovered fully from the craniotomy and underwent the subsequent sonication experiments two weeks later. The recovery time allowed for wound-healing and for the absorption of air trapped under the skin during surgery, which were confirmed by MRI taken before the sonication.

MRI-compatible sonication setup

MRI provided the anatomical as well as functional information of the brain and also was used to provide the spatial coordinates to target the FUS focus. The sonication apparatus, illustrated in Fig. 1, was integrated into a clinical 3 Tesla MRI scanner (VH; GE Medical, Waukesha, WI). The FUS transducer was mounted on the MRI-compatible 3-axis positioning system (Uni-Slides; Velmex, Bloomfield, NY) and was submerged in degassed water. A transmit/receive MR surface coil (2" diameter, constructed in-house) was located beneath the objects to be imaged in order to improve the signal-to-noise-ratio (SNR) of the MRI. Prior to positioning the animal in the sonication setup, FUS was applied to a silicone gel continuously for 2 min at an acoustic intensity of 50 W/cm^2 (spatial-peak pulse-average intensity; I_{sppa}). The silicon gel was imaged using a temperature-sensitive spin echo MRI sequence (TE/TR = 17/300 msec, echo-train-length = 4, matrix = 256×128, field-of-view (FOV) = 16×16 cm^2, slice thickness = 3 mm) five times during sonication, covering three orthogonal planes containing the focus. The temperature change in the object modulates the spin-lattice relaxation time (T_1) that is sensitive to temperature-dependent Brownian motion and consequently creates MR-signal contrast (Wlodarczyk et al., 1999). Image subtraction before and after sonication revealed the areas that were sonicated (an example is shown in the upper right inset of Fig. 2), and the coordinate of the acoustic focus was determined from the location of maximal signal contrast. After localization of the acoustic focus, the animal was laid supine on a plastic panel mounted above the system. The head was demobilized by a plastic holder and partially submerged into a hole that opened into a bag of degassed water to secure an uninterrupted path from the transducer to the targeted tissue.

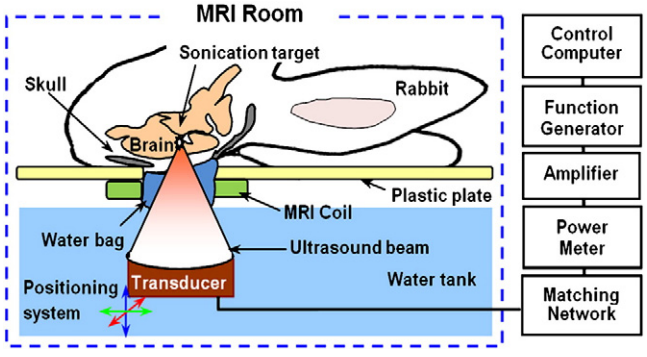

Fig. 1. Diagram of the experimental apparatus. The ultrasound transducer was mounted on the 3-axis positioning stage and submerged into degassed water. The computer-controlled operation of a function generator produced electrical signals that actuated the ultrasound transducer after being amplified by a linear radiofrequency amplifier. A power meter was used to monitor the power input to the brain.

Characterization of the FUS transducer

An air-backed, spherical segment FUS transducer (diameter = 10 cm; radius-of-curvature = 8 cm) operating at a fundamental frequency of 690 KHz was used. The relatively low frequency, compared to the frequencies used in diagnostic ultrasound imaging, is applicable to the transcranial delivery of FUS whereby the frequency range of 440–700 KHz has an optimal transmission gain through the *ex vivo* human skull (White, 2006; White et al., 2006). The transducer was actuated by a sinusoidal electrical signal generated from a function generator (Agilent Technology, Santa Clara, CA) which was amplified by a linear RF amplifier (403LA; ENI Inc., Rochester, NY). The electrical impedance of the transducer was matched to the output impedance of the amplifier by an external matching network. The acoustic power output in relation to the given power of the driving electrical signal was measured by a calibrated needle hydrophone (HNR500; Onda, Sunnyvale, CA). The hydrophone was mounted to the high-resolution 3-axis robotic stage (Bi-Slides; Velmex, Bloomfield, NY) to map the received power characteristics of acoustic fields in space covering 2.5×2.5 cm^2, with 0.5 mm steps. Measurement was made in rubber-laid degassed water bath. The acoustic intensity, as presented in I_{sppa}, was estimated by integrating the pulse intensity at its spatial maximum and dividing it by the pulse duration according to the American Institute of Ultrasound Medicine (AIUM) standards (NEMA, 2004). The spatial-peak temporal-average intensity, I_{spta}, was calculated by multiplying the duty factor of the pulse operation to the I_{sppa}. The size of the cigar-shaped acoustic focus was 2.3 mm in diameter and 5.5 mm in length, measured at full-width-at-half maximum (FWHM) of the acoustic intensity (Fig. 2). The pressure amplitude of the sonication focus was estimated after taking into account ultrasound attenuation through 5 mm of a neural tissue, with a mean attenuation coefficient of 5 Np/m/MHz (0.43 dB/cm/MHz) (Goss et al., 1978).

Mapping of target modulatory areas using fMRI

The visual and motor areas of the rabbit brain were subjected to sonication to test the neuro-modulatory potential of FUS. Since anatomical information (obtained from structural MRI) alone may not adequately provide the location of functional brain areas, real-time fMRI was employed to map the visual and motor areas of the brain. A gradient-echo (single-shot) echo-planar imaging sequence was used (TR/TE = 1500/35 msec; flip angle (FA) = 90°; matrix = 64×64; FOV = 8×8 cm^2; image matrix = 64×64; slice thickness = 3 mm; slices = 7, no gap; voxel size = $1.25\times1.25\times3$ mm^3) to image most of the brain in the axial orientation to obtain the T_2*-weighted blood-oxygenation-level-dependent (BOLD) fMRI signal. The data acquired during the initial 12 s-long period were discarded to allow for T_1 signal equilibration. We used a block-based design to deliver the

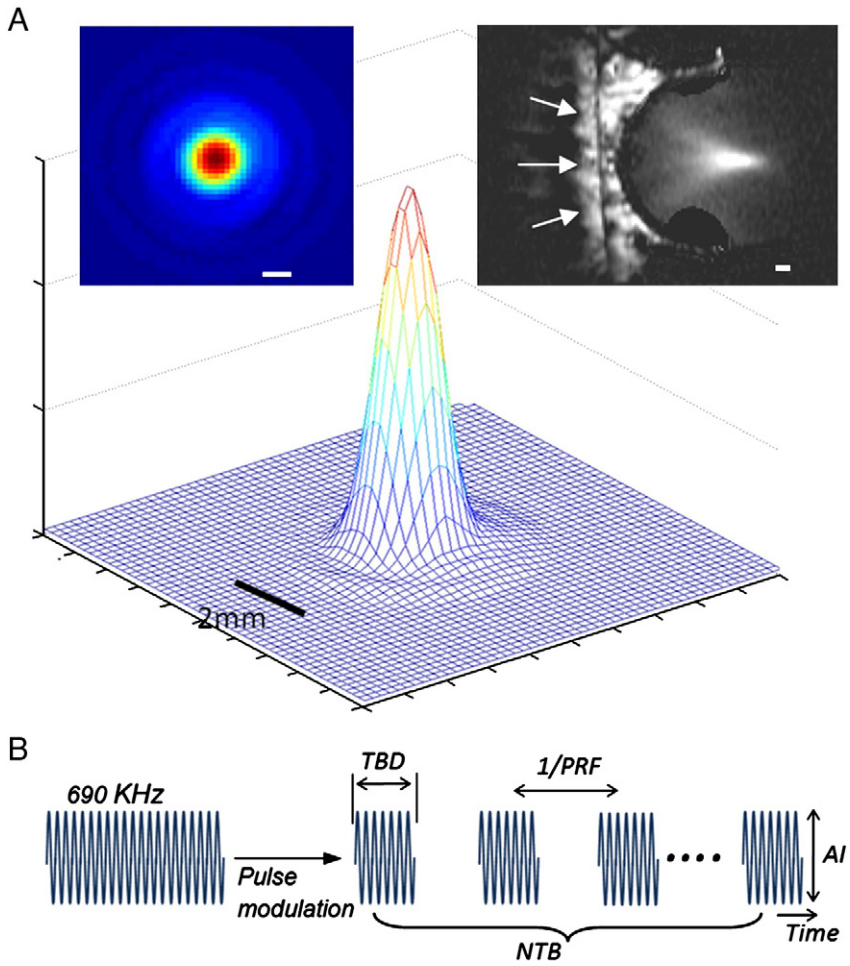

Fig. 2. (A) Three-dimensional acoustic intensity profile at the focal plane perpendicular to the sonication path (left inset, two-dimensional profile). The right inset shows the sonication profile along the sonication path (arrows) as detected in the MRI of a silicon gel after continuous sonication for 2 min at an acoustic intensity of 50 W/cm^2 (I_{sppa}). Bars indicate 2 mm. All values were normalized at the peak. (B) Illustration of sonication pulsing schemes. TBD indicates tone-burst-duration; PRF, pulse repetition frequency; AI, acoustic intensity; NTB, number of tone bursts.

interleaved periods of both "no-stimulation" and "stimulation" (each 21 s-long block). To map the rabbit's sensorimotor areas, the first joint of the right forepaw was actuated by a rod to elicit its movement of ~5 mm at 2 Hz. To detect the activity associated with visual stimulation, a strobe light (from white light-emitting diodes; LED) flashing at 4 Hz was applied to both eyes with the ambient light off. The image data were immediately transferred to an adjacent computer via a file-transfer-protocol (FTP) over the Ethernet connection, and the stimulus-related activation in the brain was identified using pixel-by-pixel temporal correlations with the canonical hemodynamic responses (Lee et al., 2008, 2009). The areas showing a temporal correlation to the given stimulation were statistically thresholded ($p<0.005$) and overlaid on anatomical images to visualize the site of activation to provide the spatial coordinates for the FUS sonication.

Test of FUS parameters for modulatory effects

A range of sonication parameters was tested under electrophysiological monitoring to assess potential modulatory effects. All measurements were conducted outside of the main MRI bore (<50 gauss) by moving the scanner table away from the center of the MRI bore to rule out potential interference from the strong magnetic field. The sonication parameters used in the experiments, as illustrated in Fig. 2, were modified using different tone burst durations (TBDs), pulse repetition frequencies (PRFs), acoustic intensities (AIs), and the number of tone bursts (NTBs) using pulse controlling software (Sonomo; SensMed, Framingham, MA). The types of the applied sonication parameters were randomized in sequence. Effort was given to find the effective sonication parameter at an AI, equal to or less than 6.4 W/cm^2 I_{sppa} (corresponds to a spatial peak negative pressure amplitude of 0.38 MPa), to minimize the potential effect of tissue damage. The corresponding mechanical index (MI), which is used based on regulatory safety guidelines for ultrasound devices, was 0.5, whereas an MI up to 1.9 is permitted for diagnostic scanners (Duck, 1999). According to the perspective of MI, the spatial peak negative pressure amplitude of 1.5 MPa can be used for a center frequency of 690 KHz.

To examine the excitatory effects of sonication on brain activity, FUS was administered to the motor area ($n=4$) as guided by the coordinates of the motor activation locus. FUS was administered at different AIs (3.3, 6.4, 9.5, and 12.6 W/cm^2 I_{sppa}), TBDs (0.05, 0.5, 10, and 50 msec), and PRFs (10, 20, 100, and 1000 Hz). The different sonication durations (0.5, 1, 1.5, and 2 s) were also achieved by modifying the NTB. The presence of cortical excitation was detected by the positive BOLD signal from the motor area. The fMRI findings were later confirmed by the induced motion of the forepaw contralateral to the sonication site, as it was measured by a pair of thin (~200 microns in diameters) silver/silver-chloride Teflon-coated subdermal disposable electrodes (SWE; Ives EEG Solution, Canada) that were inserted into the muscle of the forelimb radius and carpus. A ground electrode was positioned on the tip of the ear. The signal was

obtained at 1 KHz sampling rates using data acquisition software (LabChart 7; AD Instrument, CO).

The suppressive effect of FUS on neural activity was measured by detecting changes in the visual evoked potentials (VEP) associated with the sonication. VEP was elicited by 50 msec-long light flashes (generated by the white LED) to both eyes ($n=6$) and was obtained from the subdermal EEG electrodes (SWE; Ives EEG Solution, Canada) that were inserted under the frontal and occipital surface of the rabbit skin with a 2 cm gap. The detected EEG signals (100 measurements, taken every 500 msec) were amplified and averaged (PowerLab 8/30; AD Instrument, CO). In the measured VEP, the amplitude of positive signal deflection around 30 msec post-stimulus (noted as the "p30" component) was identified prior to sonication. Sonication was delivered to the visual areas for 18 s (administered for 9 s to each hemisphere) without light stimulation using a TBD of 0.5 msec and a PRF of 100 Hz at acoustic intensity of 3.3 W/cm^2 I_{sppa}. Upon sonication, the VEP was measured repeatedly 11 times every 1 min and 30 s to examine the post-sonication responses. The sonication parameter was determined based on the outcome of the separate rtfMRI that decreased the BOLD signal from the visual cortex during light stimulation (more than 30% reduction in its magnitude). The combinations of different PRFs (10, 20, 100, and 1000 Hz) and intensities (3.3, 6.4, and 9.5 W/cm^2 I_{sppa}) were used during this exploratory procedure. The TBD of 0.5 msec reduced the potential power deposition caused by the elongated sonication time compared to the excitatory sonication.

Examination of spatial specificity and BOLD signal dynamics from fMRI

fMRI was also used to monitor the modulation of region-specific brain activity. We examined the BOLD signal dynamics resulting from sonication to validate the physiological recordings and to further examine the intensity-dependent degree of excitation ($n=4$). Using the same imaging parameters for the detection of the sonication target, the sonication was delivered three times (starting at 27 s, with 21 s gaps between them) during the 87 s-long acquisition of fMRI (excluding the initial 12 s of dummy scans) without the presence of any external stimulation. Sonication was administered at two different acoustic intensities (i.e., 3.3 and 6.4 W/cm^2 I_{sppa}) with a 50 msec TBD and a 10 Hz PRF for a duration of 1 s. This trial-based fMRI paradigm allowed for the measurement of the amount of BOLD signal contrast originating from the sonicated areas as well as unsonicated brain areas.

To provide neuroimaging evidence for the suppression of regional cortical excitability, 9 s-long sonications were delivered to the unilateral visual cortex (the chosen hemisphere was randomized) at TBD = 0.5 msec, PRF = 100 Hz, and AI = 3.3 W/cm^2 (corresponding to the parameter that successfully suppressed the p30 VEP component) under fMRI monitoring. A total of 7 fMRI sessions were administered, once every 2 min, for each sonication experiment ($n=10$) to obtain the progression and the recovery of light-induced BOLD signal responses with respect to the sonication. The light stimulation was provided by applying white LED lights at 4 Hz to both eyes. The first session was conducted to measure the pre-sonication level of BOLD signal during light stimulation. The second session measured the BOLD signal affected by the simultaneous application of sonication. The remaining 5 fMRI sessions were administered to monitor the recovery of BOLD signal responses after the application of the FUS. In each fMRI session, 15 s and 45 s-long non-stimulus periods were added before and after the photic stimulation to establish the resting-level neural activity. We also examined whether or not sonication alone created artifactual BOLD signal contrast from the target region without visual stimulation.

For the visualization of the fMRI activation maps, the volumetric data were processed using SPM2 software using a general linear model (GLM). Motion correction and spatial smoothing (2 mm FWHM 3D Gaussian kernel) were applied, and the effect of interest was calculated for each voxel using the canonical hemodynamic response function (HRF), and subsequently thresholded at $p<0.005$ to define the areas of activation. The signal time-series obtained from the sonication site, which consists of the activation locus and 4 surrounding voxels, was scaled with respect to the baseline signal level (i.e., the first 7 volumes acquired). The time series of the BOLD signal was time-corrected and averaged across the 21 s intervals. To examine the suppressive effect, the signal time-series from the sonicated visual area was averaged between the non-stimulation periods (i.e., the first 10 and last 20 time points) and the stimulation periods (i.e., 6 time points corresponding to 9 s of stimulation). Due to the depth-varying sensitivity from the surface coil and the presence of minimal head motion (<0.5 mm spatial translation from all animals), motion correction and a spatial smoothing filter were not adopted in this part of data analysis.

MR thermometry and contrast-enhanced examination of blood brain barrier (BBB) integrity

To examine the presence of temperature modulation during sonication, tissue temperature was non-invasively measured ($n=7$) immediately after the fMRI-sonication experiment by the detection of changes in the water proton resonant frequency (wPRF) (Ishihara et al., 1995; McDannold and Jolesz, 2000). Changes in wPRF were estimated using the phase images of a fast spoiled gradient-echo (FSPGR) sequence (sequential multiphase, TE = 14 msec; FA = 30°; 256×128; bandwidth = 17.9 KHz). We acquired these temperature maps in the focal plane perpendicular to the ultrasound beam after successful functional regulation. Following the acquisition of MR thermometric data, an MRI contrast agent (Magnevist; Bayer, Wayne, NJ) was injected via ear vein, and T_1-weighted images (spin echo sequence) were obtained before and after the injection to examine the presence of BBB disruption.

Post-sonication histological analysis

Seven of the experimental animals were sacrificed immediately after the experiment (within 2 h of the start of the first sonication). Injection of Trypan Blue was used to examine the presence of BBB disruption and any acute changes in the brain tissue. The remaining animals ($n=11$) were allowed to survive for different lengths of time ($n=1$, 4 days; $n=2$, 1 week; $n=2$, 2 weeks; $n=3$, 3 weeks; $n=2$, 4 weeks, $n=1$, 6 weeks) after the FUS to monitor any adverse intermediate- or long-term biological changes associated with the procedure. The brain was extracted from all animals after the sacrifice and fixed in 10% buffered neutral formalin and embedded in paraffin. Serial sections perpendicular to the sonication beam were cut and underwent histological analysis using hematoxylin and eosin (H&E) stain to examine the presence of hemorrhaging or tissue damage. We also applied the terminal deoxynucleotidyl transferase-mediated dUTP-biotin nick end labeling (TUNEL) staining ($n=13$; ApopTag kit; Millipore, Billerica, MA) with 0.5% methyl green counter-staining to examine the signs of DNA-fragmentation, which is the early sign of tissue damage/apoptosis (Gavrieli et al., 1992). To visualize ischemic neurons, we used vanadium acid fuchsin (VAF) staining with toluidine blue counterstaining (Victorov et al., 2000) ($n=13$).

Results

Examination of the excitatory effect of FUS sonication on the motor cortex

Real-time monitoring of forepaw movement allowed for on-site adjustment of the sonication parameters. We found that only a limited fraction of the tested sonication parameters resulted in observable

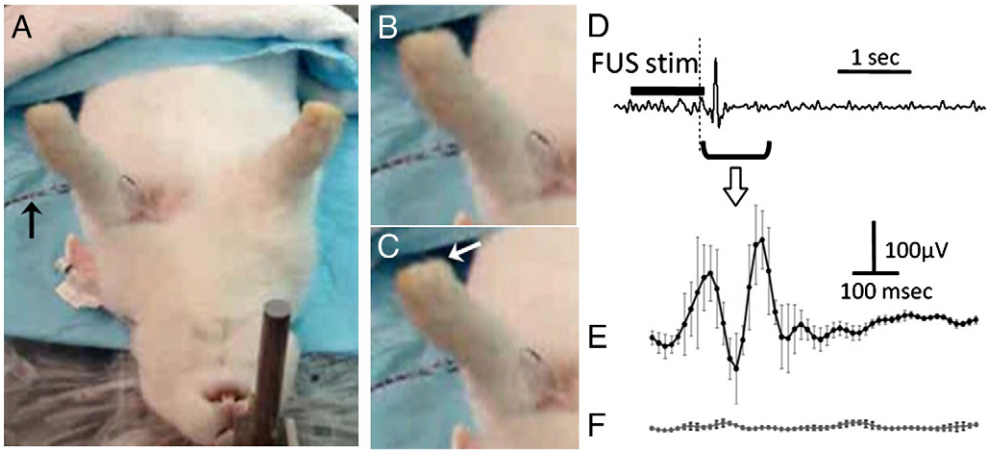

Fig. 3. (A) Experimental setup of a rabbit with subdermal electrodes positioned in the left forepaw for motion recording (see arrow). Upon sonication, forepaw movement was observed (B and C; arrow indicates movement). (D) An example of forepaw motion recording from an animal. The signal averaged across four repeated excitations (with standard error) recorded upon the completion of 1 s-long sonication in the motor cortex (E) and away from the motor cortex (F) ($n=4$).

motor activity. FUS given at TBD = 50 msec, PRF = 10 Hz, and I_{sppa} = 12.6 W/cm^2 (I_{spta} = 6.3 W/cm^2) for a duration equal to and greater than 1 s elicited motor activity detectable by both visual inspection (Fig. 3A–C) and electrophysiological recordings (Fig. 3D and E). The sonication which was given at the 2 mm caudal to the motor area of the brain did not elicit any motor activity (Fig. 3F).

fMRI confirmed the effect of sonication on rabbits. Across all animals, selective excitation of the targeted motor area was observed (an example is shown in Fig. 4). The BOLD activation was observed at a much lower acoustic intensity (I_{sppa} = 3.3 W/cm^2 with corresponding I_{spta} = 1.6 W/cm^2) compared to the intensity that resulted in forepaw movement. The crosshairs in Fig. 4A and B indicate the spatial coordinates of the sonication focus, which coincide well with the area that displayed increased BOLD signals. There was no other site of activation across the brain, which suggests the spatially-selective excitation of the motor area. The BOLD signal time-course obtained from the sonication locus (Fig. 4C) across the animals ($n=4$) confirmed that sonication, delivered at acoustic intensities of 3.3 and 6.4 W/cm^2 I_{sppa}, successfully elicited a BOLD signal increase on the order of 1.5% from the non-stimulated state, whereas an un-sonicated control site (in green line Fig. 4C) did not show such signal change.

Examination of the suppressive effect of FUS sonication on the visual cortex

The magnitude of the p30 VEP component was reduced when FUS was given at TBD = 0.5 msec, PRF = 100 Hz, AIs = 3.3 W/cm^2, and 6.4 W/cm^2 I_{sppa} for more than 7–8 s. An example of VEP recordings from an animal is shown in Fig. 5A. After sonication to the visual area of the brain, the magnitude of the p30 component was reduced from ~50 μV (Fig. 5A, black dotted line) to 10 μV (Fig. 5A, solid red line), with a reduction of signal peaks around 80 msec post-stimulus. This reduction was recovered back to the pre-sonication level 10 min after sonication (Fig. 5A, solid blue line). Based on the examination of group-level trends ($n=6$) of the p30 magnitude, which was acquired for 15 min after the FUS, the p30 component was suppressed for about 7 min before recovering back to the pre-sonication level (Fig. 5B).

This suppressive effect of the FUS on electrophysiological recordings was confirmed by fMRI mapping (Fig. 6). Sonication of the visual cortex (TBD = 0.5 msec, PRF = 100 Hz, I_{sppa} = 3.3 W/cm^2, I_{spta} = 160 mW/cm^2) suppressed the regional cortical activity (Fig. 6A, middle row). However, the activation detected during the pre-sonication fMRI was recovered by the second post-sonication

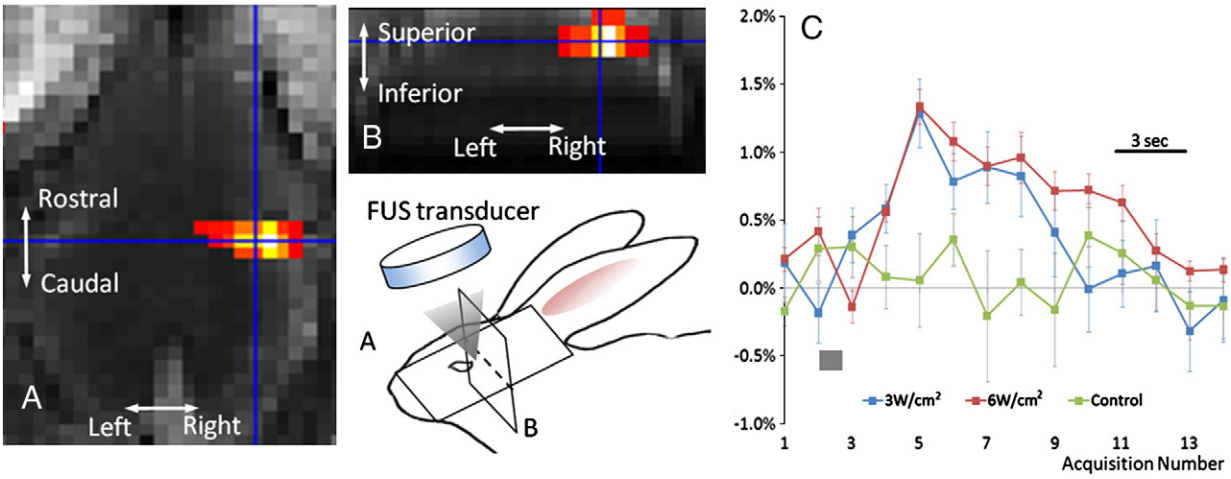

Fig. 4. (A and B) fMRI activation maps showing selective FUS-mediated activation of the somatomotor area in the right cerebral hemisphere (visualized using a threshold of $p<0.005$). Spatial orientation is illustrated in the cartoon (inset). The crosshairs on the fMRI map indicate the location of the sonication focus. (C) FUS-mediated BOLD signal time course (percentage BOLD signal change) from the sonication focus ($n=4$; with standard error) for two different acoustic intensities (3.3 and 6.4 W/cm^2 I_{sppa}). The BOLD signal from the unsonicated control site is shown in green line. The gray bar indicates the timing of the sonication.

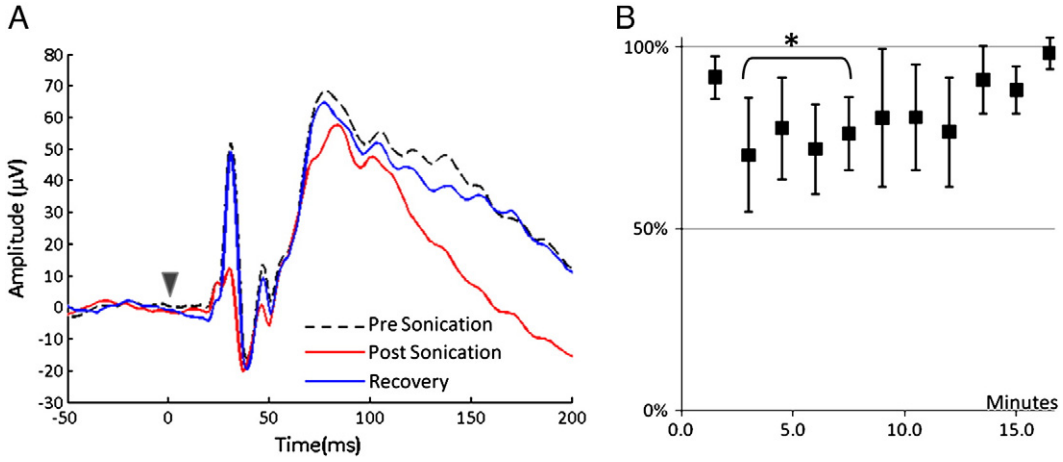

Fig. 5. (A) VEP recordings from an animal. The pre-sonication baseline VEP activity is shown as a black dotted line. VEP after the application of FUS to the visual areas is shown as a solid red line, and the recovery of VEP 10 min after the sonication, is shown as a solid blue line. The gray arrow indicates the timing of visual stimulation. (B) Changes in the magnitude of the p30 component, normalized with respect to the pre-sonication level ($n=6$; with standard error). * indicates a significant difference from the pre-sonication level (paired t-test; $p<0.05$).

fMRI session (Fig. 6A, bottom row). The examination of the BOLD signal contrast across the sessions also revealed that the BOLD contrast (~1.2% change) elicited by the visual stimulation from the sonicated visual area was reduced during the sonication and remained suppressed for another fMRI session (Fig. 6B, blue bars). The BOLD contrast obtained from the unsonicated visual area was unaltered throughout the sessions (Fig. 6B, red bars). Sonication alone, without the presence of visual stimulation, did not elicit any BOLD signal from the visual area (Fig. 6B, green bars). The duration of the suppressive effects after the 9 s of sonication was similar between the findings from VEP (p30 magnitude) and fMRI (BOLD signal contrast), whereby approximately 10 min were needed to recover to the baseline pre-sonication levels.

MR thermometry

As shown in Fig. 7, MR thermometry ($n=7$) showed that there was no measurable temperature change even during the 27 s long continuous application of the FUS at the site of focus (comparing pre-, during, and post- sonication periods; paired t-test; all, *n.s.*). The sensitivity of the employed MR thermometry method, as determined by the measurement of signal fluctuation in the absence of the sonication, was 0.3 ± 0.06 °C. This suggests that the thermal mechanism did not contribute to the observed modulation of BOLD signal. Short duration application (1 s) of a much higher AI ($I_{sppa}=12.6$ W/cm^2) that was required to produce the visible forepaw movement also did not generate any measurable temperature change. The longer (27 s) duration of sonication at a much higher AI ($I_{sppa}=23$ W/cm^2; $I_{spta}=1.15$ W/cm^2) produced only a slight temperature increase (~0.7 °C) in the sonicated area.

Post-sonication histological analysis and MRI contrast enhancement

Histological analysis did not show the presence of tissue damage associated with the sonication in any of the animals (Fig. 8, for example). No anatomic damage was found in the H&E sections. Neither TUNEL positive apoptotic cells nor VAF positive ischemic cells were found in the examined sections. The animals that were allowed

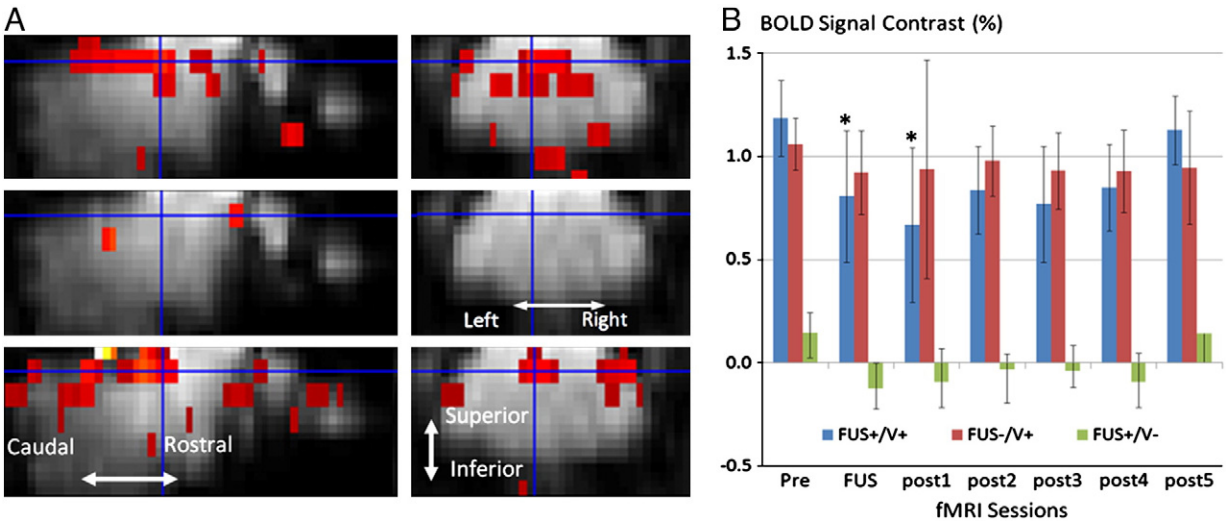

Fig. 6. (A) Changes in the fMRI map of visual activity (thresholded at $p<0.005$) from before (top row) and after sonication (middle row), along with the map showing recovery of pre-sonicated activity (bottom row). (B) The suppression of group-averaged ($n=10$) BOLD signal upon the application of FUS and its recovery (noted "FUS+/V+"; * indicates a significant reduction at $p<0.05$). The unsonicated sites (FUS−/V+) did not show any reductions in BOLD contrast level. The sonication alone did not elicit any BOLD signal from the sonicated site ("FUS+/V−"). x-axis labels: pre indicates pre-sonication; FUS, during sonication; post 1 through 5, post-sonication periods.

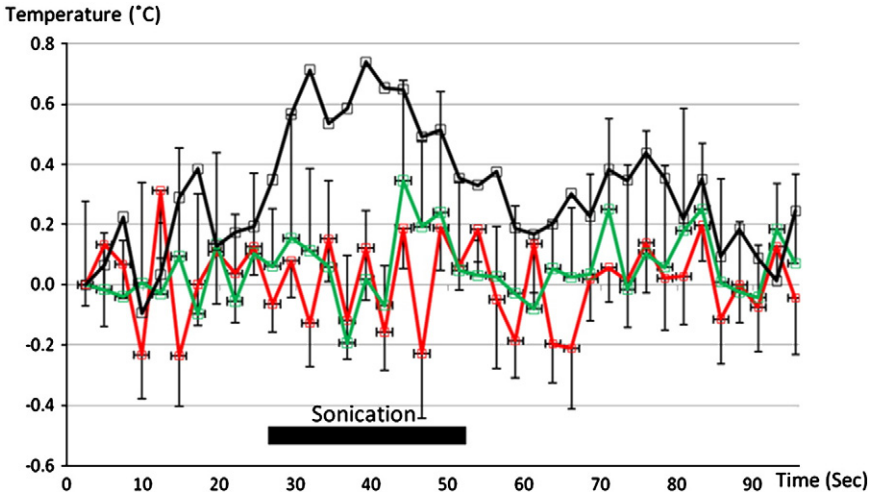

Fig. 7. Tissue temperature measured using MR thermometry from the sonication locus (red line) and the control non-sonicated site (green line) ($n=7$; shown with standard error). The sonication duration is shown by a black bar. The black solid line indicates that a slight temperature rise (less than 0.8 °C) was detected when higher acoustic intensity ($I_{sppa}=23$ W/cm^2) was given at the same pulsing scheme (i.e., TBD = 0.5 msec and PRF = 100 Hz; $I_{spta}=1.15$ W/cm^2).

to survive after the experiment also showed normal behavior, including normal eye tracking of food in the visual field of both eyes. The contrast-enhanced analysis of the sonicated regions ($n=5$) showed that there was no significant difference between sonicated and unsonicated areas in terms of the degree of MR signal enhancement caused by the injection of the gadolinium contrast agents (enhancement of $15\pm8\%$ and $16\pm8\%$ for the sonicated and unsonicated areas, respectively), suggesting that the BBB was not disrupted by the given sonication conditions.

Discussion

There has been long standing interest in using FUS to modulate neuronal activity by delivering anatomically targeted acoustic energy to a localized region in the brain. The results presented here demonstrate the evidence of FUS-mediated regional modulation of neural tissue excitability *in vivo*. The modulatory effects were bimodal, whereby the brain activity can be stimulated and selectively suppressed. The effects were confirmed by both electrophysiological

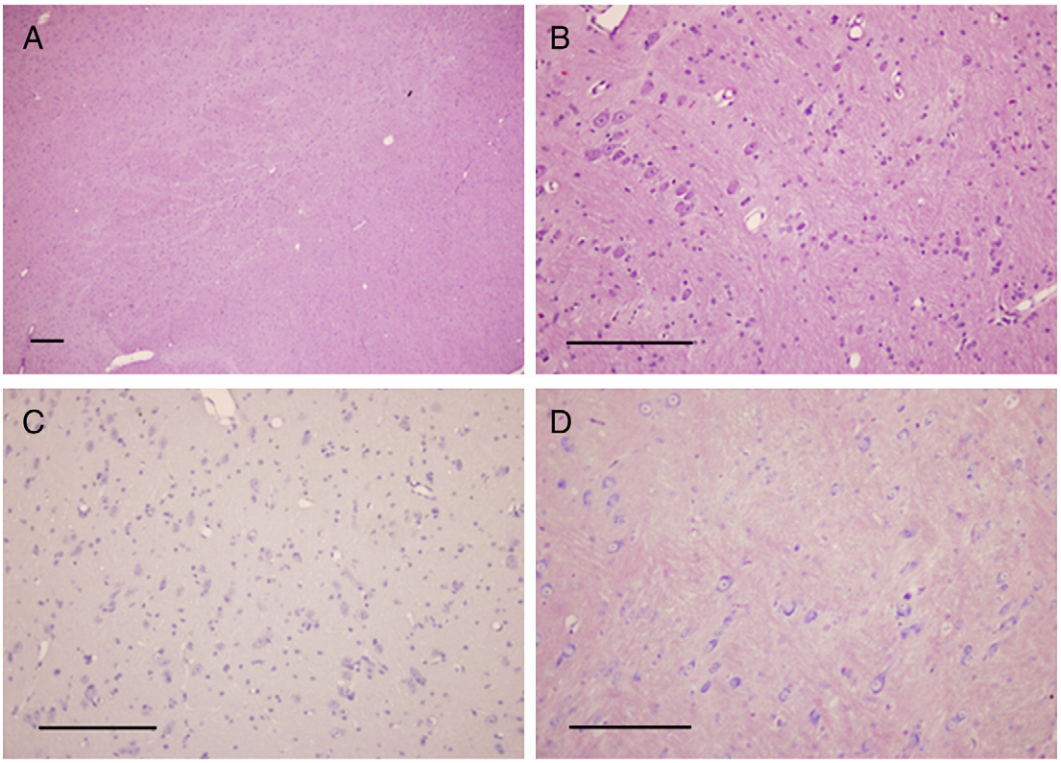

Fig. 8. Histological examination of the sonicated rabbit brain. H&E stained tissue section at magnification (A) 4× and (B) 20×. Sonication did not cause any visible minor or major vascular damage. Magnified (20×) view of (C) TUNEL and (D) VAF stained sections of the rabbit's brain (black bars, 150 μm). No TUNEL positive, apoptotic cells are present. No major ischemic alteration, like acidophilic cells, were found in the VAF stained sections.

recordings and fMRI. MRI guidance was crucial not only to localize the targeted modulatory area but also to precisely deliver the acoustic focus to its target. With the advent of the multi-arrayed FUS transducer design with independent control of the directional acoustic phase (Clement et al., 2005; Hynynen and Jolesz, 1998; White, 2006), spatially-steerable, transcranial delivery of high-intensity FUS in the human brain became feasible using a commercial system (Martin et al., 2009; McDannold et al., 2010). Therefore, although the current study involved the removal of the skull to accurately quantify the level of sonication, the translation of the presented technique for application through the intact skull will not carry significant technical barriers.

Modulation of excitability in neural tissue

Among the combinations of TBD and PRF, we found that only a limited scope of the tested sonication parameters was shown to be effective in achieving the desired neuromodulation. We observed that a TBD of 50 msec given at a PRF of 10 Hz elicited the contra-lateral motor activity and associated BOLD signal responses. The sonication time, which is determined by the number of tone bursts (NTB), also seemed to play an important role in the observed increase in BOLD signal. For example, sonication durations equal to or longer than 1 s (i.e., requiring greater than 10 NTBs) were needed. The acoustic intensity needed to elicit an excitatory effect was 1.6 W/cm^2 I_{spta} (3.3 W/cm^2 I_{sppa}), which was significantly greater than the range in which Tufail et al. (2010) elicited the motor response in mice (i.e., less than 180 mW/cm^2) using a non-focused pulsed application of the ultrasound beam. The cause for this discrepancy still requires further investigation; however, we conjecture differences in the study designs, type of animal, state of anesthesia, transducer frequency, and the choice of ultrasound transducer (i.e., focused versus unfocused) might have contributed to the discrepancy. Further systematic testing covering a wider range of sonication parameters at different fundamental frequencies is also needed to establish the relationship between the sonication parameters and the degree of modifiable excitability in the neural tissue.

fMRI mapping of the neuronal excitation induced by the FUS revealed that the site of excitation coincided well with the site of sonication. This is indicative of selective neuro-modulation achieved by the FUS. The local excitation of the neural tissue of the motor cortex was confirmed by its direct stimulation and subsequent manifestation of forepaw movement. We hypothesize that increased AI up to 12.6 W/cm^2 (I_{sppa}), which was much higher than the AI required for the observed BOLD response, is associated with the generation of sufficient descending cortico-spinal volleys to depolarize spinal alpha motor neurons and recruit sufficient muscle units to elicit gross limb movement. Since the posture of the limb as well as its relation to gravity affect motor movement from cortical excitation, detection of more subtle electromyography (EMG) activity, e.g., motor evoked potential (MEP), along with spinal neurophysiologic recordings, would be needed to elaborate on our findings. We also found that FUS, administered at a shorter TBD of 0.5 msec, PRF of 100 Hz, and AI of 3.3 W/cm^2 (I_{spta} = 160 mW/cm^2; 5% duty cycle), suppressed the visual activity induced by the light stimulation, as measured by VEP (i.e., suppression of the p30 component). This suppressive effect lasted a few minutes after the sonication. This observation strikingly resembles work by Fry et al. (1958) whereby the EEG was monitored from a cat when ultrasound (unfocused) was directed to lateral geniculate nucleus.

Potential mechanisms behind the observed neuromodulation

Several hypothetical scenarios can be suggested regarding the potential mechanism underlying modulatory effects on cortical excitability. One scenario would be the mechanical movement of neural tissue by ultrasound in a strong static magnetic source (such as MRI) and subsequent induction of electrical currents (by Lorentz forces) that in turn stimulate the nerve tissue (Norton, 2003). Although a part of the experiment was conducted under MR guidance, our electrophysiological findings, which were obtained virtually outside the main MRI field, suggest that involvement of the strong magnetic field in the observed neuromodulatory effects can be ruled out. Secondly, temperature changes could also contribute to modulatory changes in neural cell excitability whereby an increase in tissue temperature could reduce its excitability (Colucci et al., 2009). Based on MR thermometry results, the modulatory effects were observed in the absence of temperature changes at the sonication focus even at a much longer duration of sonication (i.e., 27 s). This suggests that the observed effects were likely to be traced to the non-thermal, mechanical movements of the local brain tissue. Although the precise mechanism behind the observation has not been elucidated, stretch-sensitive ion channels of the neurons may be involved (Morris and Sigurdson, 1989; Rinaldi et al., 1991). The non-thermal modulation of voltage-gated sodium and calcium channels by short bursts of low-intensity (I_{sppa} = <3 W/cm^2) ultrasound has been demonstrated by Tyler et al. (2008). Further experiments, for example, using neuropharmacologic manipulation with channel blockers, are needed to address the fundamental mechanism behind the FUS-mediated neural excitation.

It is notable that FUS can also be used to suppress neural activity. Stimulation-related cortical activity of the visual area was suppressed using a much shorter sonication pulse duration (0.5 msec) applied at a higher frequency (100 Hz PRF) compared to the excitatory sonication while using an equivalent acoustic intensity (I_{sppa} = 3.3 W/cm^2). The time-averaged acoustic intensity (I_{spta} = 160 mW/cm^2) was also 10 times smaller than those used in excitatory sonication (I_{spta} = 1.6 W/cm^2). We hypothesize that relatively long exposure of FUS to neural tissue (on the order of a few seconds or minutes), which is divided into shorter pulses (thus reducing the duty cycle and associated time-averaged intensity), can render neurons less excitable. Since the acoustic focus used in this study was relatively large compared to the rabbit brain anatomy, excitation of an inhibitory network in the visual cortex or disruption of nerve conduction in the optic tract cannot be completely ruled out. It is also notable that effects of FUS leading to excitation may be very different from those leading to the suppression of neural activity. For example, excitation would require the elicitation of action potentials, whereas the suppression may be limited to blocking neural signal conduction. A study at the cellular level of the neural tissue, both central and peripheral nervous system, including the use of voltage-sensitive dyes or direct measurement of trans-membrane potential, would provide a more detailed mechanism behind our observation.

Biological safety of FUS sonication

Both histological analysis and MR contrast enhancement imaging showed that the tested sonication parameters did not cause brain tissue damage at variable time-points after sonication. Our findings support that low intensity sonication with a small negative peak pressure amplitude (0.38 MPa at 6.4 W/cm^2 I_{sppa}) did not cause the BBB to be disrupted. This corresponds to an MI of 0.5, which is much lower than the current FDA limit for soft tissue US (1.9) (Duck, 1999) and is far less than the MI range that would cause BBB disruption or cavitation. The sonication intensity that suppressed the neural activity (less than 320 mW/cm^2 I_{spta}) was far less than the current FDA-regulatory limit on most clinical ultrasound imagers (I_{spta} = 720 mW/cm^2), with the exception of obstetrical applications (I_{spta} = 96 mW/cm^2) (AIUM-Committee, C.S, 2004).

Future clinical applications

The ability to modulate localized neural activation can ultimately be used as a completely new functional brain mapping method that

permits the study of brain connectivity in a much more elegant and non invasive way than was possible until now. For example, anatomically and functionally targeted sonications may also offer selective and reversible suppression of white matter tracts. Diffusion-tensor MRI (e.g., DTI) only offers anatomical information related to white matter connectivity (Catani and Thiebaut de Schotten, 2008; Yoo et al., 2005). Temporary conduction blocks imposed on white matter fibers by FUS and their effect on cortical functions will provide an unprecedented opportunity in the direct assessment of white matter activities that are implicated in brain injuries.

The neuromodulatory potential of FUS can also be used in conjunction with functional neurosurgery, whereby FUS induces lesions in pathologic neural circuits (for example, thalamatomy for treating pain, epilepsy, and movement disorders) (Martin et al., 2009). Prior to complete ablation, the function of targeted brain areas can be systematically assessed by the application of FUS and concurrent intra-procedural cognitive evaluations. The modulatory effect would only be transient, and thus the particular brain regions affected by FUS sonication can be identified in one session and ablated during subsequent procedures. Other than this imminent potential clinical application, we anticipate that the FUS-mediated modulation of neuronal activity may also open new avenues of clinical applications for the treatment of various neurological and psychiatric illnesses.

Acknowledgments

The authors gratefully acknowledge the support of the Focused Ultrasound Surgery Foundation, NARSAD, the Center for Integration of Medicine and Innovative Technology (to S.S. Yoo), and the Gerald J and Dorothy R Friedman Foundation for Medical Research (to S.S. Yoo and A. Bystritsky). We also acknowledge support from NARSAD (Woody Wurster Distinguished Investigator Award to A. Bystritsky), the National Center for Research Resources, and the Harvard Clinical and Translational Science Center (UL1 RR025758) and NIH grant K24 RR018875 (to A. Pascual-Leone). The authors thank the editorial support from Matthew Marzelli.

Disclosure: Alexander Bystritsky is a founder and a stockholder of Brainsonix, a California corporation.

References

AIUM-Committee, C.S, 2004. How to interpret the ultrasound output display standard for higher acoustic output diagnostic ultrasound devices: version 2. J. Ultrasound Med. 23, 723–726.

Catani, M., Thiebaut de Schotten, M., 2008. A diffusion tensor imaging tractography atlas for virtual in vivo dissections. Cortex 44, 1105–1132.

Clement, G.T., White, P.J., King, R.L., McDannold, N., Hynynen, K., 2005. A magnetic resonance imaging-compatible, large-scale array for trans-skull ultrasound surgery and therapy. J. Ultrasound Med. 24, 1117–1125.

Colucci, V., Strichartz, G., Jolesz, F., Vykhodtseva, N., Hynynen, K., 2009. Focused ultrasound effects on nerve action potential in vitro. Ultrasound Med. Biol. 35, 1737–1747.

Dalecki, D., 2004. Mechanical bioeffects of ultrasound. Annu. Rev. Biomed. Eng. 6, 229–248.

Duck, F.A., 1999. Acoustic saturation and output regulation. Ultrasound Med. Biol. 25, 1009–1018.

Foster, K.R., Wiederhold, M.L., 1978. Auditory responses in cats produced by pulsed ultrasound. J. Acoust. Soc. Am. 63, 1199–1205.

Fregni, F., Pascual-Leone, A., 2007. Technology insight: noninvasive brain stimulation in neurology-perspectives on the therapeutic potential of rTMS and tDCS. Nat. Clin. Pract. Neurol. 3, 383–393.

Fry, F.J., Ades, H.W., Fry, W.J., 1958. Production of reversible changes in the central nervous system by ultrasound. Science 127, 83–84.

Gavrieli, Y., Sherman, Y., Ben-Sasson, S.A., 1992. Identification of programmed cell death in situ via specific labeling of nuclear DNA fragmentation. J. Cell Biol. 119, 493–501.

George, M.S., Aston-Jones, G., 2010. Noninvasive techniques for probing neurocircuitry and treating illness: vagus nerve stimulation (VNS), transcranial magnetic stimulation (TMS) and transcranial direct current stimulation (tDCS). Neuropsychopharmacology 35, 301–316.

Goss, S.A., Johnston, R.L., Dunn, F., 1978. Comprehensive compilation of empirical ultrasonic properties of mammalian tissues. J. Acoust. Soc. Am. 64, 423–457.

Hoy, K.E., Fitzgerald, P.B., 2010. Brain stimulation in psychiatry and its effects on cognition. Nat. Rev. Neurol. 6, 267–275.

Hynynen, K., Jolesz, F.A., 1998. Demonstration of potential noninvasive ultrasound brain therapy through an intact skull. Ultrasound Med. Biol. 24, 275–283.

Ishihara, Y., Calderon, A., Watanabe, H., Okamoto, K., Suzuki, Y., Kuroda, K., 1995. A precise and fast temperature mapping using water proton chemical shift. Magn. Reson. Med. 34, 814–823.

Jolesz, F.A., Hynynen, K., McDannold, N., Tempany, C., 2005. MR imaging-controlled focused ultrasound ablation: a noninvasive image-guided surgery. Magn. Reson. Imaging Clin. N. Am. 13, 545–560.

Lee, J.H., O'Leary, H.M., Park, H., Jolesz, F.A., Yoo, S.S., 2008. Atlas-based multichannel monitoring of functional MRI signals in real-time: automated approach. Hum. Brain Mapp. 29, 157–166.

Lee, J.H., Ryu, J., Jolesz, F.A., Cho, Z.H., Yoo, S.S., 2009. Brain–machine interface via real-time fMRI: preliminary study on thought-controlled robotic arm. Neurosci. Lett. 450, 1–6.

Magee, T.R., Davies, A.H., 1993. Auditory phenomena during transcranial Doppler insonation of the basilar artery. J. Ultrasound Med. 12, 747–750.

Martin, E., Jeanmonod, D., Morel, A., Zadicario, E., Werner, B., 2009. High-intensity focused ultrasound for noninvasive functional neurosurgery. Ann. Neurol. 66, 858–861.

McDannold, N., Clement, G.T., Black, P., Jolesz, F., Hynynen, K., 2010. Transcranial magnetic resonance imaging-guided focused ultrasound surgery of brain tumors: initial findings in 3 patients. Neurosurgery 66, 323–332 discussion 332..

McDannold, N.J., Jolesz, F.A., 2000. Magnetic resonance image-guided thermal ablations. Top. Magn. Reson. Imaging 11, 191–202.

Morris, C.E., Sigurdson, W.J., 1989. Stretch-inactivated ion channels coexist with stretch-activated ion channels. Science 243, 807–809.

NEMA, 2004. Acoustic Output Measurement Standard for Diagnostic Ultrasound Equipment.

Norton, S.J., 2003. Can ultrasound be used to stimulate nerve tissue? Biomed. Eng. Online 2, 1.

Rinaldi, P.C., Jones, J.P., Reines, F., Price, L.R., 1991. Modification by focused ultrasound pulses of electrically evoked responses from an in vitro hippocampal preparation. Brain Res. 558, 36–42.

Tufail, Y., Matyushov, A., Baldwin, N., Tauchmann, M.L., Georges, J., Yoshihiro, A., Tillery, S.I., Tyler, W.J., 2010. Transcranial pulsed ultrasound stimulates intact brain circuits. Neuron 66, 681–694.

Tyler, W.J., Tufail, Y., Finsterwald, M., Tauchmann, M.L., Olson, E.J., Majestic, C., 2008. Remote excitation of neuronal circuits using low-intensity, low-frequency ultrasound. PLoS ONE 3, e3511.

Victorov, I.V., Prass, K., Dirnagl, U., 2000. Improved selective, simple, and contrast staining of acidophilic neurons with vanadium acid fuchsin. Brain Res. Brain Res. Protoc. 5, 135–139.

Wagner, T., Valero-Cabre, A., Pascual-Leone, A., 2007. Noninvasive human brain stimulation. Annu. Rev. Biomed. Eng. 9, 527–565.

White, P.J., 2006. Transcranial focused ultrasound surgery. Top. Magn. Reson. Imaging 17, 165–172.

White, P.J., Clement, G.T., Hynynen, K., 2006. Local frequency dependence in transcranial ultrasound transmission. Phys. Med. Biol. 51, 2293–2305.

Wlodarczyk, W., Hentschel, M., Wust, P., Noeske, R., Hosten, N., Rinneberg, H., Felix, R., 1999. Comparison of four magnetic resonance methods for mapping small temperature changes. Phys. Med. Biol. 44, 607–624.

Yoo, S.S., Park, H.J., Soul, J.S., Mamata, H., Park, H., Westin, C.F., Bassan, H., Du Plessis, A.J., Robertson Jr., R.L., Maier, S.E., Ringer, S.A., Volpe, J.J., Zientara, G.P., 2005. In vivo visualization of white matter fiber tracts of preterm- and term-infant brains with diffusion tensor magnetic resonance imaging. Invest. Radiol. 40, 110–115.